NANO: Brief Reports and Reviews
Vol. 3, No. 1 (2008) 45–50

World Scientific
www.worldscientific.com

FEW WALLED CARBON NANOTUBE PRODUCTION IN LARGE-SCALE BY NANO-AGGLOMERATE FLUIDIZED-BED PROCESS

QIANG ZHANG*, HAO YU, YI LIU, WEIZHONG QIAN, YAO WANG, GUOHUA LUO and FEI WEI†
Beijing Key Laboratory of Green Reaction Engineering and Technology
Department of Chemical Engineering, Tsinghua University
Beijing, 100084, P. R. China
**zhang-qiang@mails.tsinghua.edu.cn*
†*weifei@flotu.org*

Received 12 November 2007
Revised 5 December 2007

Few walled carbon nanotubes (FWCNTs) have been successfully synthesized using a nano-agglomerate fluidized-bed process. FWCNTs can be obtained by fluidization of Fe(Co/Ni)/Mo/MgO catalysts at a high temperature with methane cracking in a nano-agglomerate fluidized-bed reactor. The products were mainly 2 to 5 walled CNTs with an outer diameter of 1–7 nm in high purity, as revealed by Raman spectrometry, SEM, and HRTEM analysis. Two keys were crucial for this process. The first key was to get the small size of activity catalyst particles which was realized by Mo addition in catalyst. The graphitization of FWCNTs strongly depended on the composition of catalyst. Fe/Mo/MgO catalyst showed the highest activity and the FWCNT product with the best graphitization. Another key for this process was that the particles must be kept in fluidized state during FWCNT formation. Detailed process information was reported in this article, which showed a potential way for the large scale production of FWCNTs, thereby the urgent need for FWCNTs in high performance will be overcome.

Keywords: Few walled carbon nanotube; fluidized bed; large scale.

1. Introduction

As a new type of carbon materials, various demands for carbon nanotubes (CNTs) were put forward for different potential applications, including conductive and high-strength composites, sensors, field emission displays, transparent conductive film, and nanometer-sized semiconductor devices. Single-walled CNTs (SWCNTs) show good performance in super reinforced composite materials.[1] But until now, it is still not easy to produce SWCNTs cost-effectively in large scale. Lukic reported that few walled CNTs (FWCNTs) had similar mechanical properties to SWCNTs. Unlike SWCNTs, even after covalent functionalization, FWCNTs can keep the structural integrity of their inner tubes, thus, they are expected to be a better candidate for polymer reinforcement than either SWCNTs or the more defective multi-walled CNTs (MWCNTs).[2] Another studies indicated that the smaller the diameter of CNTs was, the better property of the field emission due to the large field enhancement factor.[3] Compared with other types of nanotubes, FWCNTs have enhanced field emission characteristics with lower threshold field and improved emission stability, due to their perfect structure.[4]

Although FWCNTs are unique intermediates that can solve some problems of SWCNTs and MWCNTs, they also introduced their own list of problems that need to be solved, before they can be used in commercial applications. The large scale production to get FWCNTs on kilogram scale is one of the major problems. Chemical vapor deposition (CVD) method was the most foreground way for CNT synthesis because of the low cost and high yield.[5–23] Various catalysts, such as Co/Mo, Co/V, and Co/Fe on zeolite or corundum alumina, have been used to obtain CNTs in fixed beds.[7] Recently, Qian *et al.* reported that high quality FWCNTs can be synthesized over Co/Mo/MgO and Co/W/MgO.[8] Also Fe/Mo/MgO and Ni/Mo/MgO were effective to synthesize FWCNTs in the furnace operated as a fixed bed.[9,10] Qi *et al.* reported that the ethanol/methanol mixture was better for FWCNT synthesis.[12] Fixed beds were widely used for this process since they were easy to be built up and operated.[7–12] But FWCNTs on gram or milligram scale were synthesized in fixed beds, because the increasing volume of CNTs would jam the reactor at high CNT yield. The fluidized bed reactor provides an expanding space and uniform temperature distribution, thus is potential in mass production of CNTs.[13–23] So far, the researches related to producing CNTs in fluidized beds mainly concerned with the large scale synthesis of SWCNTs or MWCNTs.[16–23] Here we report a nano-agglomerate fluidized bed process to large scale produce FWCNTs from methane.

2. Experimental Details

2.1. *Catalyst preparation*

The M/Mo/MgO (M = Fe, Co and Ni) catalyst was prepared by a coprecipitation method. Typically, the solution of $Mg(NO_3)_2 \cdot 6H_2O$ and $M(NO_3)_x \cdot yH_2O$ was precipitated with the solution containing $(NH_4)_2CO_3$ and $(NH_4)_6Mo_7O_{24} \cdot 4H_2O$ at 293–353 K. After filtering, drying and calcination, the resulting solids were ground to fine catalyst powders. Further details of the preparation of the catalyst are given in Ref. 24.

2.2. *Carbon nanotube synthesis*

To synthesize the FWCNTs, approximate 10 g of the catalyst was sprayed uniformly into a quartz fluidized bed reactor (i.d. 50 mm, height 1000 mm as shown in Fig. 1). A sintered quartz disk (porosity 15–44 lm) as the gas distributor was sealed halfway along its length. The quartz fluidized bed reactor, mounted in an electrical tube furnace, was then heated to 600°C, in an air atmosphere. Subsequently, argon was fed at a flow rate of 1800 ml/min and the H_2 was introduced into the reactor at 600°C at a rate of 150 ml/min for 3 min for reducing the catalyst. After reduction, the reactor temperature was increased to 900°C. Then a mixture of CH_4/H_2 (300/150 ml/min, v/v) was introduced into the fluidized bed reactor for 1 h.

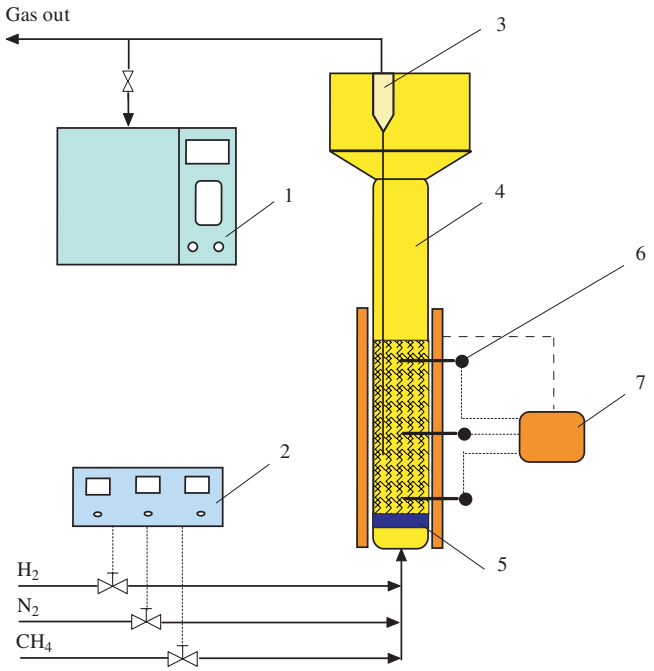

Fig. 1. Schematic representation of the nano-agglomerate fluidized bed for FWCNTs synthesis. 1 — gas chromatogram; 2 — mass flow controller; 3 — cyclone; 4 — fluidized-bed reactor; 5 — gas distributor; 6 — thermocouple; 7 — heat controller.

2.3. *Characterization*

The morphology of the FWCNT was characterized by a JSM 7401F high resolution scanning electron microscope (SEM) operated at 5.0 kV and a JEM 2010 high resolution transmission electron microscope (TEM) operated at 120.0 kV. Scattering Raman characterization of the CNTs was obtained using a Raman microscope (Renishaw, RM2000, He–Ne laser excitation line at 633.0 nm) at ambient conditions. TGA (TGA-2050) was used to characterize the purity of the FWCNTs.

3. Results and Discussion

For the synthesis of FWCNTs, the property of catalyst is an intrinsically crucial factor. According to the vapor–liquid–solid model, it is important to control the sizes of active sites responsible for the CNT growth at high temperature. If large particles form, the diameters of CNTs will increase.[25] Generally, the methods to disperse metal nanoparticles on the supports include tailoring the loading of metal,[26] using organic solvents as protecting agents in the preparation,[27] assisting with other compositions,[28] forming a stable uniform phase on molecular level,[25] and phase separation effect.[29,30] Among them, due to the advantage of easy realization, low cost and high reliability, Mo is usually added into the catalyst to limit the diameters of CNTs. Since the characteristics of CNT products significantly varied with the active constitute of catalysts, the catalyst effect on the FWCNT production is first discussed.

SEM observation was performed to investigate the morphology of the as-grown products synthesized in the fluidized bed. Typical SEM images were shown in Fig. 2. Abundant fibrous products, forming interwoven coverage, grew densely at the synthesis temperature of 900°C over Fe/Mo/MgO, Co/Mo/MgO and Ni/Mo/MgO catalysts with molar ratios of 3:1:96. The diameters of the CNTs grown on all the catalysts were less than 10 nm.

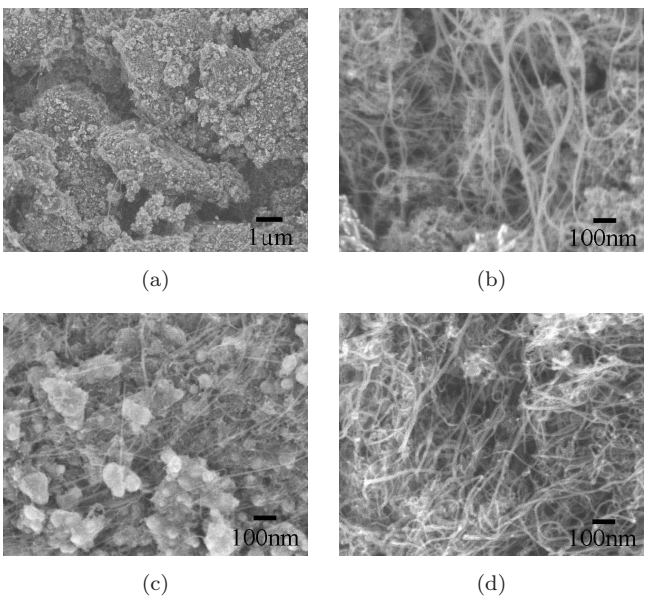

Fig. 2. SEM images of the FWCNTs grown in the fluidized bed. (a) Low magnification image of the Co/Mo/MgO catalyst product. (b)–(d) The high magnification images of the Co/Mo/MgO, Fe/Mo/MgO, and Ni/Mo/MgO catalyst products.

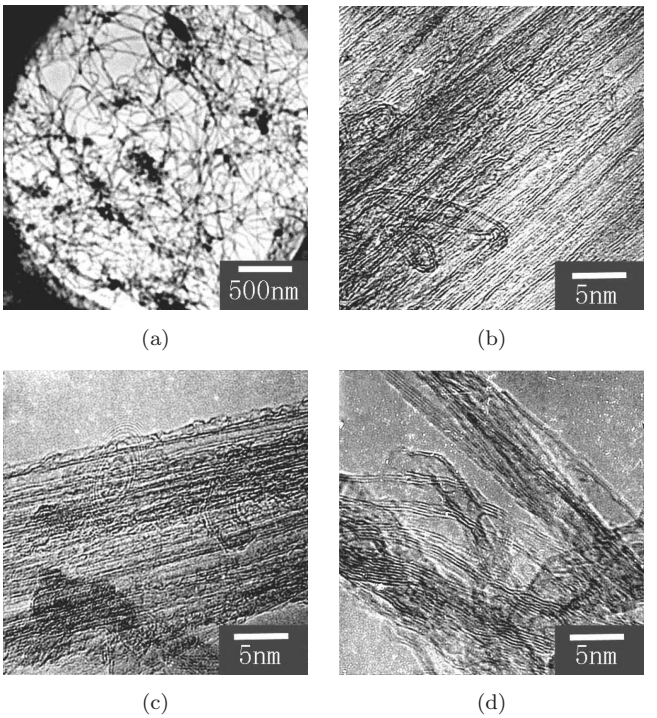

Fig. 3. TEM images of the FWCNTs grown in the fluidized bed. (a) Low magnification image of the Co/Mo/MgO catalyst product. (b)–(d) The high magnification image of Co/Mo/MgO, Fe/Mo/MgO, and Ni/Mo/MgO catalyst products.

The formation of the FWCNTs was further confirmed by the observation of TEM, as shown in Fig. 3. These FWCNTs were in bundles of diameter about 10–25 nm. Only little amorphous carbon in these samples was observed, as shown in Figs. 2 and 3. Main impurities were particle-like catalysts consisted of mainly MgO. They can be easily removed by acid (such as HCl). Furthermore, the formation of FWCNTs was demonstrated by the presence of radial breath modes (RBMs) in the low wave number region (100-300 cm^{-1}) of Raman spectra (Fig. 4).

Although FWCNTs were obtained over different catalysts in the fluidized bed reactor, their yields and structural characteristics varied with catalysts significantly. The CNT yield, defined as the mass ratio of FWCNTs grown to the active metal on catalyst from TGA results, is shown in Table 1. All the catalysts showed high yields over 15 to the metal catalyst, indicating that FWCNT products with purities of 90 to 97% can be obtained only by washing with dilute acid to remove MgO. Thus, the fluidized bed technique is potential for the production of FWCNTs in high purity. Among the catalysts used in this work, the

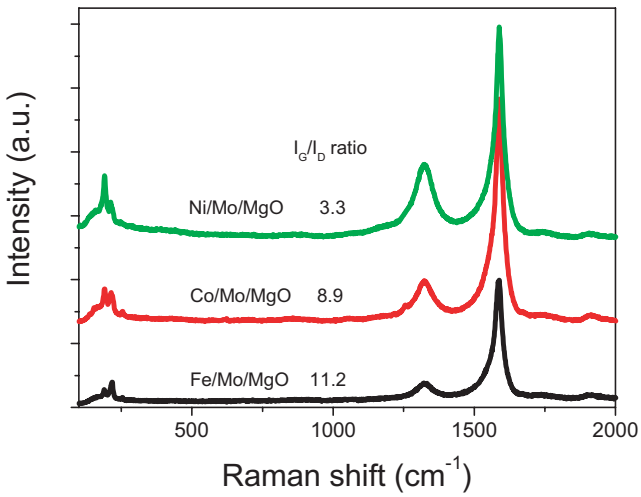

Fig. 4. Raman spectra of the products from Fe/Mo, Co/Mo and Ni/Mo catalysts supported on MgO.

Table 1. The yield, diameter and graphitization of the as-grown FWCNTs from M/Mo/MgO (M = Fe, Co, Ni)

Catalyst M/Mo/MgO	Fe	Co	Ni
FWCNT yield	34.6	27.8	16.2
Average inner diameter/nm	1.1	1.2	1.5
Average outer diameter/nm	2.5	2.7	3.8
I_G/I_D ratio	11.2	8.9	3.3

Fe/Mo/MgO catalyst gave the highest yield, while the Ni/Mo/MgO catalyst gave the lowest one. The sizes of the FWCNTs obtained from these catalysts were estimated with HRTEM images from about 40 FWCNTs and is listed in Table 1. The FWCNTs from Fe/Mo/MgO catalyst were with the narrowest diameters, while the Ni/Mo/MgO catalyst showed the largest diameters. These statistical results were consistent with Raman spectra representing the collective behaviors of samples, as shown in Fig. 4. These spectra show the typical spectroscopic characteristics of FWCNTs, as characterized by the strong G band (tangential mode) around 1580 cm^{-1}, the weak D band (related to disordered graphite or amorphous carbon) at 1335 cm^{-1}, and the presence of sharp RBMs in the low wave number region (100–300 cm^{-1}). For the FWCNTs in a bundle form, the diameter of CNT shell was calculated with the relationship d (nm) = 232 (cm^{-1}nm)/(ω − 6.5) (cm^{-1}). It was a mixture of 2–5 walls for FWCNTs, and was difficult to obtain the diameter of a specify CNTs. The I_G/I_D ratios, reflecting the graphitization of CNTs, varied with the type of catalysts from 3 to 11.2. The I_G/I_D ratio of FWCNTs from Fe/Mo/MgO was 11.2, indicating the best graphitization of CNTs. All the I_G/I_D ratios were higher than 3 and similar to that of SWCNTs.[31]

The above results demonstrated that the catalyst effect was obvious, even for the product from the nano-agglomerate fluidized bed reactor (NAFBR). This was caused by the different dispersion of metal catalyst. Commonly, Fe/MgO was a good catalyst for S/DWCNTs.[25,26,28,29] When Mo element was added into the catalyst, due to the formation of FeMo alloys, the distribution of diameter will be widened. The Co/Mo/MgO also show similar phenomena. For Ni/Mo/MgO, due to the high activity of carbon cracking and carbon solubility,[32] the CNTs grown from Ni/Mo/MgO always showed a little larger diameter. The products from the NAFBR also confirmed this point. So the catalyst effect was also validated in the NAFBR process for FWCNTs production. If better catalysts were used, such as Co/W/MgO and Fe/W/MgO, better FWCNT might be obtained.[8]

The catalyst effect was obvious in the FWCNT production. But the reason for that the FWCNTs can also be produced in the NAFBR, was the agglomerated structure of the CNT/catalyst composite. The FWCNTs are of the diameter of 1–7 nm, the length of 0.1–1000 μm, with the aspect ratio more than several thousands, which cannot be described correctly using Geldart particles classification. However, as shown in Fig. 2, due to the FWCNTs have only a few walls, they are very flexible and easy to grow along the pore of the catalysts. Some CNTs can link various catalysts loosely and keep them in the aggregating state. The aggregating properties of FWCNTs and catalysts particles,[16–18,33] as shown in Fig. 2(a) have given us the chance to successfully synthesize FWCNTs with the CCVD process in a fluidized bed reactor. Both the catalyst and the as-grown product can be easily fluidized. The technology of nano-agglomerates fluidized in the MWCNTs production process was realized.[16–18,31]

Another interesting phenomena was the FWCNTs can be formed into a ring structure as shown in Fig. 5. The ring is in a diameter of 600 nm and with a thickness of about 20 nm. This nanostructure was obtained without other processes and detailed analysis can be obtained in Refs. 34–39. One of the possible ways to form a CNT crystal is by coiling a CNT or small bundle into a ring. Due to the energy barrier, the activation energy must be

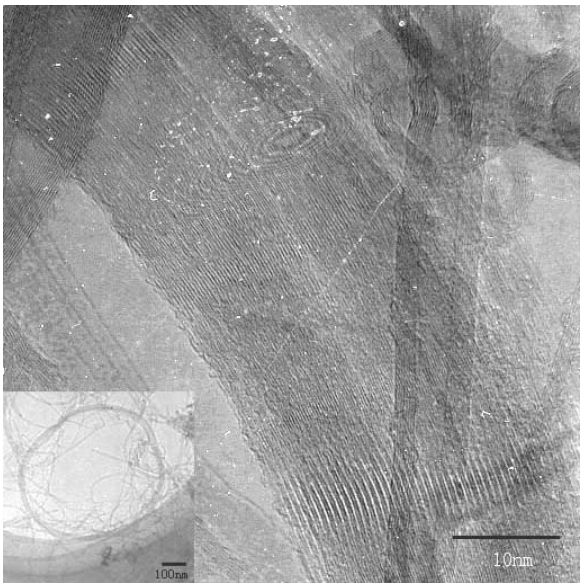

Fig. 5. Transmission electron microscopy images of the FWCNT ring grown from Fe/Mo/MgO catalyst in the fluidized bed.

provided, usually by ultrasonic irradiation, to coil or bend the one-dimensional nanotube bundle to form a highly curved circle. In our process, the as-grown product was movable in the reactor and the gas flow can provide such activation energy.[37] Also the confinement in the catalyst pores provides a situation allowing the bending and coiling of the CNT bundles. However, the exact formation mechanism is not yet well understood, thus further researches are needed to make sure the relationship between the fluidized bed operation and the formation of FWCNT ring structure.

4. Conclusions

FWCNTs can be grown by the NAFBR technique, in a controllable manner using Fe(Co, Ni)/Mo/MgO catalysts. The products are mainly 2 to 5 walled CNTs with an outer diameter of 1–7 nm in high purity. FWCNTs from Fe/Mo/MgO catalyst are the best crystalline with the fewest defects, while the CNTs from the Ni/Mo/MgO catalyst come with larger diameter and more defects. Mo can segregate the activity catalyst particle and is one of crucial factors for FWCNT formation. Both the catalyst and the product were in an agglomerate state and provide the possibility to scale up this process. In some cases, FWCNT ring structure was found in the as-grown product. This approach offers multiple advantages over the common fixed bed process, such as uniform gas–solid mixture and avoidance of catalyst particle sintering, and shows promise for the large-scale, potentially continuous, production of FWCNTs, at high yield. Then we can get a large-scale production of FWCNTs with Fe(Co, Ni)/Mo/MgO catalysts by fluidize bed process. If other materials, such as zinc oxide, silicon, Ge, iron oxide, and GaAs, can be formed into agglomerate structure with a diameter of several tens micrometers, then they also can be produced with NAFBR in future.

Acknowledgments

The work was supported by the Natural Scientific Foundation of China (Nos. 20736004 and 20736007), China National Program (No. 2006-CB0N0702), and Key Project of Chinese Ministry of Education (No. 106011).

References

1. A. B. Dalton, S. Collins, E. Munoz, J. M. Razal, C. H. Ebron, J. P. Ferraris, J. N. Coleman, B. G. Kim and R. H. Baughman, *Nature* **423**, 703 (2003).
2. B. Lukic, J. W. Seo, R. R. Bacsa, S. Delpeux, F. Beguin, G. Bister, A. Fonseca, J. B. Nagy, A. Kis, S. Jeney, A. J. Kulik and L. Forro, *Nano Lett.* **5**, 2074 (2005).
3. N. de Jonge, M. Allioux, M. Doytcheva, M. Kaiser, K. B. K. Teo, R. G. Lacerda and W. I. Milne, *Appl. Phys. Lett.* **85**, 1607 (2004).
4. C. Qian, H. Qi, B. Gao, Y. Cheng, Q. Qiu, L. C. Qin, O. Zhou and J. Liu, *J. Nanosci. Nanotechnol.* **6**, 1346 (2006).
5. R. H. Baughman, A. A. Zakhidov and W. A. de Heer, *Science* **297**, 787 (2002).
6. J. W. Seo, A. Magrez, M. Milas, K. Lee, V. Lukovac and L. Forro, *J. Phys. D: Appl. Phys.* **40**, R109 (2007).
7. I. Willems, Z. Konya, J. F. Colomer, V. G. Tendeloo, N. Nagaraju, A. Fonseca and J. B. Nagy, *Chem. Phys. Lett.* **317**, 71 (2000).
8. C. Qian, H. Qi and J. Liu, *J. Phys. Chem. C* **111**, 131 (2007).
9. H. J. Jeong, K. K. Kim, S. Y. Jeong, M. H. Park, C. W. Yang and Y. H. Lee, *J. Phys. Chem. B* **108**, 17695 (2004).
10. L. P. Zhou, K. Ohta, K. Kuroda, N. Lei, K. Matsuishi, L. Z. Gao, T. Matsumoto and J. Nakamura, *J. Phys. Chem. B* **109**, 4439 (2005).
11. C. G. Lu and J. Liu, *J. Phys. Chem. B* **110**, 20254 (2006).
12. H. Qi, C. Qian and J. Liu, *Chem. Mater.* **18**, 5691 (2006).

13. C. E. Baddour and C. Briens, *Int. J. Chem. Reactor Eng.* **3**, R3 (2005).
14. C. Vahlas, B. Caussat, P. Serp and G. N. Angelopoulos, *Mater. Sci. Eng. R* **53**, 1 (2006).
15. S. H. Chee and H. T. Andrew, *Ind. Eng. Chem. Res.* **46**, 997 (2007).
16. Y. Wang, F. Wei, G. H. Luo, H. Yu and G. S. Gu, *Chem. Phys. Lett.* **364**, 568 (2002).
17. W. Z. Qian, F. Wei, Z. W. Wang, T. Liu, H. Yu, G. H. Luo, L. Xiang and X. Y. Deng, *AIChE J.* **49**, 619 (2003).
18. Y. Hao, Q. F. Zhang, F. Wei, W. Z. Qian and G. H. Luo, *Carbon* **41**, 2939 (2003).
19. Y. L. Li, L. A. Kinloch, M. S. P. Shaffer, J. F. Geng, B. Johnson and A. H. Windle, *Chem. Phys. Lett.* **384**, 98 (2004).
20. C. B. Xu and J. Zhu, *Nanotechology* **15**, 1671 (2004).
21. H. Yu, Q. Zhang, Q. F. Zhang, Q. X. Wang, G. Q. Ning, G. H. Luo and F. Wei, *Carbon* **44**, 1706 (2006).
22. A. Morançais, B. Caussat, Y. Kihn, P. Kalck, D. Plee, P. Gaillard, D. Bernard and P. Serp, *Carbon* **45**, 624 (2007).
23. S. Y. Son, D. H. Lee, S. D. Kim, S. W. Sung, Y. S. Park and J. H. Han, *Korean J. Chem. Eng.* **23**, 838 (2006).
24. W. Z. Qian, H. Yu, F. Wei, Q. F. Zhang and Z. W. Wang, *Carbon* **40**, 2968 (2002).
25. G. Q. Ning, F. Wei, Q. Wen, G. H. Luo, Y. Wang and Y. Jin, *J. Phys. Chem. B* **110**, 1201 (2006).
26. Q. W. Li, H. Yan, Y. Cheng, J. Zhang and Z. F. Liu, *J. Mater. Chem.* **12**, 1179 (2002).
27. Y. M. Li, W. Kim, Y. G. Zhang, M. Rolandi, D. W. Wang and H. J. Dai, *J. Phys. Chem. B* **105**, 11424 (2001).
28. S. M. Huang, Q. Fu, L. An and J. Liu, *Phys. Chem. Chem. Phys.* **6**, 1077 (2004).
29. Q. Wen, W. Z. Qian, F. Wei, Y. Liu, G. Q. Ning and Q. Zhang, *Chem. Mater.* **19**, 1226 (2007).
30. Q. Zhang, W. Z. Qian, Q. Wen, Y. Liu, D. Z. Wang and F. Wei, *Carbon* **45**, 1645 (2007).
31. W. Z. Qian, T. Liu, F. Wei and H. Y. Yuan, *Carbon* **41**, 1851 (2003).
32. W. Z. Qian, T. Liu, Z. W. Wang, H. Yu, Z. F. Li, F. Wei and G. H. Luo, *Carbon* **41**, 2487 (2003).
33. H. Yu, Q. F. Zhang, G. S. Gu, Y. Wang, G. H. Luo and F. Wei, *AIChE J.* **52**, 4110 (2006).
34. J. Liu, H. J. Dai, J. H. Hafner, D. T. Colbert, R. E. Smalley, S. J. Tans and C. Dekker, *Nature* **385**, 780 (1997).
35. R. Martel, H. R. Shea and P. Avouris, *Nature* **398**, 299 (1999).
36. J. F. Colomer, L. Henrard, E. Flahaut, G. Van Tendeloo, A. A. Lucas and P. Lambin, *Nano Lett.* **3**, 685 (2003).
37. L. Song, L. J. Ci, L. F. Sun, C. H. Jin, L. F. Liu, W. J. Ma, D. F. Liu, X. W. Zhao, S. D. Luo, Z. X. Zhang, Y. J. Xiang, J. J. Zhou, W. Y. Zhou, Y. Ding, Z. L. Wang and S. S. Xie, *Adv. Mater.* **18**, 1817 (2006).
38. Z. P. Zhou, D. Y. Wan, Y. Bai, X. Y. Dou, L. Song, W. Y. Zhou, Y. J. Mo and S. S. Xie, *Physica E* **33**, 24 (2006).
39. H. Yu, Q. F. Zhang, G. H. Luo and F. Wei, *Appl. Phys. Lett.* **89**, 223106 (2006).